

Rydberg State Ionization by Half-Cycle-Pulse Excitation: Strong Kicks Create Slow Electrons

A. Wetzels,¹ A. Gürtler,¹ L. D. Noordam,¹ F. Robicheaux,² C. Dinu,¹ H. G. Müller,¹
M. J. J. Vrakking,¹ and W. J. van der Zande¹

¹*Fom Institute for Atomic and Molecular Physics, Kruislaan 407, 1098 SJ Amsterdam, The Netherlands*

²*Department of Physics, Auburn University, Auburn, Alabama 36849*

(Received 7 August 2002; published 19 December 2002)

The asymptotic velocity distribution of electrons ionized in half-cycle-pulse excitation of high Rydberg states ($n = 34$), placed in a static electric field, is studied using electron velocity-map imaging. At weak half-cycle pulse strengths, the electrons escape over the saddle point in the potential. For strong half-cycle pulses, the electrons are emitted in the direction of the field kick. The much slower and less intense half cycle of opposite polarity, which necessarily follows the main half-cycle pulse, strongly affects the momentum distribution and reduces the excess energy of the electrons significantly.

DOI: 10.1103/PhysRevLett.89.273003

PACS numbers: 32.30.-r, 32.60.+i, 32.80.-t

New developments in the generation of ultrashort pulses have enabled researchers to study a wide variety of new phenomena in Rydberg atoms. It has become possible to generate ultrashort so-called half-cycle pulses (HCP) with a frequency spectrum in the THz regime [1]. If the pulse duration of the HCP is much shorter than the classical round-trip time of the Rydberg electron, the interaction of the HCP with the Rydberg electron can be described as a momentum kick [2–6]

$$\Delta \mathbf{p} = - \int \mathbf{F}(t) dt, \quad (1)$$

where $\mathbf{F}(t)$ is the electric field of the HCP. In this limit, the resulting energy transfer is given by

$$\Delta E = \mathbf{p}_0 \cdot \Delta \mathbf{p} + \frac{1}{2} \Delta p^2, \quad (2)$$

where \mathbf{p}_0 is the initial momentum of the electron. An HCP does not propagate freely in space, as the time integral of the electric field is zero in the far field. In fact, an HCP consists of a very short main half cycle, followed by a long half-cycle pulse of opposite polarity of much smaller amplitude such that the integral of both half-cycle parts is equal. The latter half-cycle pulse is called “the tail” in the remainder. Tielking *et al.* [7] showed that this long negative tail can reduce the ionization efficiency. Wesdorp *et al.* [8] found suppression of ionization for very high Rydberg states ($n > 70$), if the electron orbit time is much longer than the duration of the full cycle pulse, further called FCP. In this regime, the change in momentum equals $\Delta p \approx 0$. Otherwise, effects of the FCP have not been described. In this Letter, we focus on the ionization of Rydberg states of xenon with energies very close to that of the saddle point in the potential created by the Coulomb field and an external static electric field. Excitation of the Rydberg states takes place in the n -mixing regime, where we excite an incoherent superposition of several k states. Classically, the external homogeneous electric field will make the

Rydberg states undergo oscillations in the orbital angular momentum, l . Hence, the HCP that follows the formation of the Rydberg state interacts with a mixture of electronic angular momentum states. Velocity-map imaging [9] is used to determine the asymptotic momentum distributions in the two directions perpendicular to the static electric field. The polarization of the half-cycle pulse is perpendicular to the static electric field. The experiments are complemented by classical calculations. The measurements and calculations show that the slow and weak tail following the HCP does not affect the ionization probabilities but influences the momentum and energy distribution of the free electrons, nullifying the energy gain from the main HCP. Our finding is illustrated in Fig. 1.

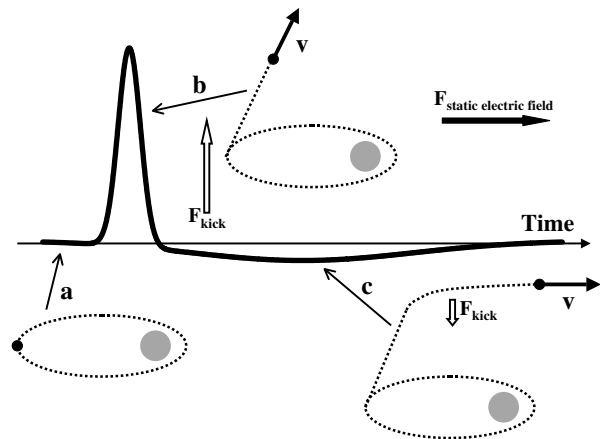


FIG. 1. Illustration of the influence of the weak tail of the HCP on the momentum distribution of the ionized electron. The kick of the HCP is shown by the white arrows. (a) Initially, the electron is in a high Rydberg state. (b) The main HCP generates electrons with a high velocity in the direction of the kick (the velocity of the electron is shown by the black arrow). (c) The tail of the HCP, which induces a weaker force on the electron but over a longer time range, reduces the velocity in the direction (anti)parallel to the kick to almost zero. The static electric field accelerates the electron towards the detector.

The initial HCP, because of its short duration, creates electrons with significant momentum/velocity in the direction of the kick. The tail transfers the same amount of momentum but in the opposite direction and reduces the momentum of the free electrons.

Figure 2 shows the experimental setup. In our experiment, metastable xenon atoms in the $^3P_{J=2}$ state are produced in an electron-impact source [10]. The outer electron, an s electron, is excited further using pulsed nanosecond UV radiation to Rydberg levels about 3 cm^{-1} below the saddle point in a static (220 V cm^{-1}) electric field. The UV polarization is in the x direction. The electric field is in the z direction. After 500 ns, an HCP is generated by illuminating a GaAs wafer with intense light of 100 fs duration from a regeneratively amplified Ti-sapphire laser. The strength of the HCP is changed using the bias voltage over the GaAs wafer. The HCP is polarized along the x axis, while its direction is changed by inverting the polarity over the wafer. The kick direction refers to the direction of the force as felt by the electron, which is opposite to the electric field vector of the HCP. The HCP measures about 1 ps; the tail has an estimated duration of 10 to 20 ps. The HCP excitation takes place in the source region of a velocity-map imaging setup [9]. The imaging apparatus consists of an extraction region containing two electrodes, which create a static electric field to accelerate the electrons into a 50 cm long field-free time of flight tube towards a microchannel-plate detector followed by a phosphor screen. The very-low-energy electrons are affected by the combined Coulomb and electric field [11,12]. The final perpendicular momentum may be established only as far as $10 \mu\text{m}$ away from the ionic core. Since the static electric field in this experiment has a significant effect on the xenon atoms as evidenced by the Stark structure, a symmetry axis parallel to the detector does not exist. As a consequence, the velocity distribution of the z component cannot be reconstructed by, for example, a so-called

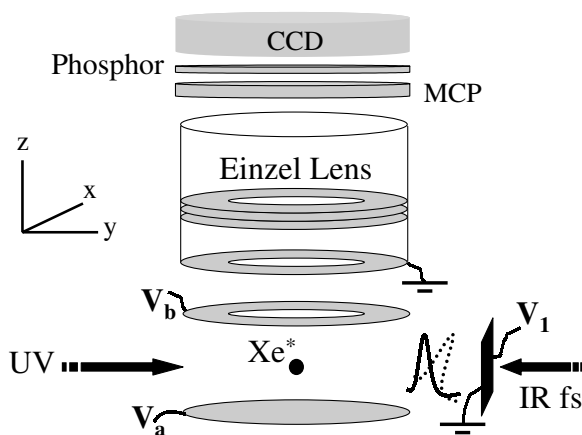


FIG. 2. Illustration of the experimental setup. See text for details.

Abel inversion procedure. A second electrostatic lens was installed to magnify the image of the very-low-energy electrons on the detector [13]. Individual electrons were detected using a point finding routine. Each image is the sum of 4000 shots. The strength of the HCP excitation and the momentum or velocity scale in the x and y directions of the images were calibrated in independent experiments. The strength of the HCP pulses was determined using field-free ionization of $n = 35$ Rydberg states. In the impulsive kick limit, at 50% ionization by the HCP the energy transferred, $\frac{1}{2} \Delta p^2$, equals the binding energy [3]. The observed displacements, Δx and Δy , of the electrons on the detector are expressed in the asymptotic (perpendicular) momentum, p_x and p_y , by performing near-threshold photoionization based on experiments by Nicole *et al.* [12]. Analytical calculations provide the relation between the displacement of the photoionized electrons on the detector and their asymptotic perpendicular momentum [11]. In this paper, we present data at various strengths of the half-cycle pulse monitoring both the total ionization yields and the momentum distributions, as a function of the transferred momentum Δp .

In Rydberg state HCP ionization classical calculations agree well with quantum calculations [5,14]. The quantum nature of the Rydberg system is taken into account in the choice of the initial conditions. The dye laser excites p -type states with $m_l = \pm 1$. We selected the initial angular momentum in the Rydberg state to be $l = 1$ with projections $-1 < l_z (= m) < 1$. The orientation of the major axis of the elliptic orbit is chosen randomly and the electron is launched at the inner turning point. The angular momentum l is not a conserved quantity in a static electric field and its value oscillates between $l = 1$ and $l = n - 1$. The HCP is chosen to interact with the Rydberg electron randomly in time covering a full oscillation of the orbital angular momentum. The calculations provide ionization efficiencies and velocity-map images.

We will first discuss the dependence of the ionization yield on the HCP strength. Figure 3 shows the experimentally observed ionization yield along with the result of the classical calculations. The ionization yield, as determined by integration of each image, is plotted against the momentum transfer. Saturation of the ionization signal for values of Δp above 0.06 a.u. was used as evidence for 100% ionization. The experimental points are the average of kicks in the positive and negative x direction, which gave the same result as expected from symmetry considerations. The measured curve does not show the S -curve dependence that is often seen [2,5]. Because of the very small binding energy of the Rydberg state in the present experiment, ionization already starts at very small HCP strengths obscuring the S -curve behavior. The experimental data are compared with classical calculations. Electrons ionize only if their energy is above the saddle point energy ($E_{el} > E_{sp}$). These electrons can be subdivided into three categories:

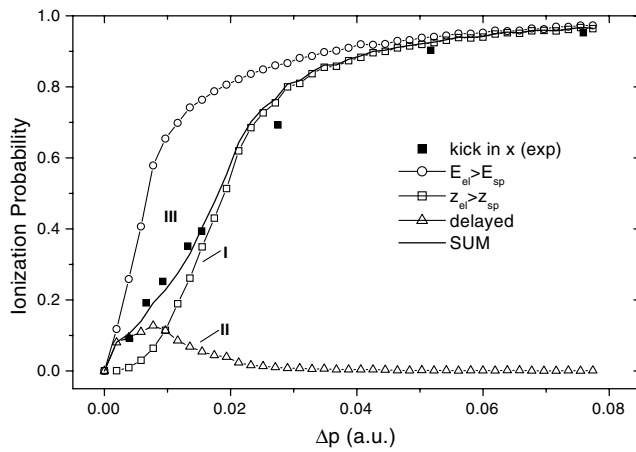


FIG. 3. Measured and calculated ionization curves versus momentum kick for polarization of the HCP perpendicular to the electric field. Three different contributions are shown in the calculation: (I) electrons which ionize directly after the HCP kick, (II) delayed ionized electrons, which ionize after scattering from the core in the direction of the saddle point, and (III) metastable electrons.

(I) electrons found downstream from the saddle point ($z_{el} > 4z_{sp}$ with the origin at the nucleus) in the classical trajectory calculations; these so-called direct electrons escape immediately: (II) electrons which did not escape independent of the calculation time but had a magnetic quantum number $|l_z|$ with $|l_z| < 1$. We assume that these electrons, called delayed electrons, will still ionize after core scattering [15]: (III) all other electrons, which did not escape over the saddle point and had $|l_z| > 1$. Figure 3 shows that the experimental curve is accurately described by the sum of direct electrons (I) and the delayed electrons (II). In a multielectron system such as xenon, electrons with a small value of $|l_z|$ undergo core scattering, conserving the value of $|l_z|$. This process may redirect the electrons towards the saddle point. The discrepancy between the observed ionization yield and the calculated yield based on the total energy of the excited atoms (open circles) leads us to conclude that some xenon atoms are formed in quasibound levels with lifetimes of several μs (III). The metastability is partially due to the excitation of large $|l_z|$ values, which enhances the centrifugal potential, keeping the electron away from the electric field axis and which raises the threshold field. Small variations in the assumed HCP width (1 ps full width at half maximum) have no effect on the calculated results. The relevant parameter is the integral over the electric field. Importantly, we find the calculated ionization curves to be identical using a HCP and a FCP.

The measured velocity-map images are symmetric at low kick strengths. The asymptotic electron momentum distributions are equal in the directions parallel and perpendicular to the kick. At high kick strength, the images are elongated in the x direction, showing that the electrons are ejected with a larger momentum parallel

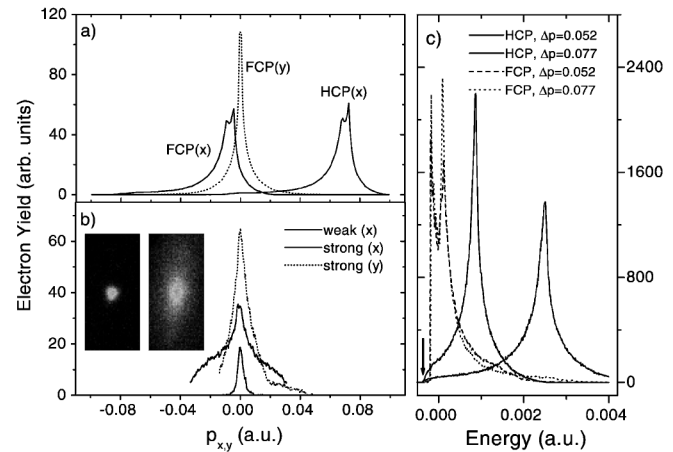


FIG. 4. (a) Calculated momentum p_x distributions for strong ($\Delta p = 0.077$) kick of both a HCP and FCP, and p_y distribution for strong FCP. (b) Measured momentum distributions in the x direction for both a weak ($\Delta p = 0.004$) and strong ($\Delta p = 0.076$) kick and in the y direction only for a strong kick. The images at low (left) and high (right) kick strengths are shown in the inset. (c) Calculated energy distributions, for $\Delta p = 0.077$, and, additionally $\Delta p = 0.052$. The energy is related to the field-free ionization threshold. The saddle point energy is indicated by an arrow.

to the HCP polarization than perpendicular to it [see Fig. 4(b)]. In the y direction, the images are symmetric. When the HCP is polarized in the z direction, the p_x and p_y momentum distributions are symmetric and highly similar to the p_y distribution in the case of perpendicular kick [14]. Figures 4(a) and 4(b) show experimental and calculated momentum distributions. In the inset, the original images are shown. Momentum differences as small as $\Delta p = 0.005$ a.u. ($v = 1.1 \times 10^4$ m/s for an electron) can be resolved at these settings. At a small kick strength, the asymptotic velocities in the x (and y) direction are small [Fig. 4(b), gray solid line]: $p_x < 0.007$ a.u. Figure 3 reveals that, at this low kick strength, the ionization yield can be explained only invoking a delayed ionization involving core scattering (II). This process may well take at least an oscillation period of the angular momentum, about 35 ps under our circumstances. The resulting asymptotic momentum distribution does not reveal the direction of the momentum kick of the HCP. Electrons excited just above the saddle point escape through the small opening angle in the Coulomb potential if their momentum in the direction perpendicular to the electric field is small. The Coulomb potential still reduces some momentum from the x (and y) directions narrowing the distribution on the detector [12]. At higher kick strengths, to our initial surprise, the p_x distribution is still centered close to zero perpendicular momentum. The maximum in the distribution seems to shift slightly to the direction opposite to the kick. The classical calculations reveal the origin of the small momentum change. A true HCP gives a significantly displaced momentum

distribution [grey solid line in Fig. 4(a)]. However, the tail shifts the distribution back without changing its shape. Hence, while the HCP gives the electron a substantial amount of kinetic energy, the tail of the FCP takes away the kinetic energy. Intense HCP ionization is a source of very low kinetic energy electrons. The momentum reduction by the tail is slightly larger than the momentum gain by the HCP, because during the second part of the pulse no kinetic energy has to be transformed into potential energy to ionize. This explains a shift opposite to the kick direction. Although we find that the observed shape is wider and less pronounced than the calculated shape, both the position and asymmetry are reproduced. The y distribution is still symmetric. We noticed that at high kick strengths the images suffer some loss of resolution due to electronic noise from the HCP generation on the ion optics. Even in the absence of this noise, the finite resolution of our detection system would hamper the observation of the splitting in the p_x distribution. The effect of the FCP character is clearly revealed from the final total energy distributions for two high kick strengths, $\Delta p = 0.052$ and $\Delta p = 0.077$ [see Fig. 4(c)]. The main HCP generates free electrons with a high kinetic energy depending on the kick strength, whereas subsequently the weak tail cancels this energy gain quantitatively and independently of the kick strength. The energy distribution after the FCP reflects the localization of the electrons in blue Stark states, located on the “uphill” side of the potential, and electrons located on the “downhill” side near the saddle point, near their turning points. The combination of high angular momentum, l , with small projection along the electric field, l_z results in this localization. After the kick electrons escape in the direction of the kick perpendicular to the electric field, not over the saddle point. During the ionization process, electrons in the blue Stark states transform more of the gained kinetic energy into potential energy than the red Stark states. The combination of the Coulomb field and the static field results in a deeper potential well for “blue” electrons. The tail effectively removes the kinetic energy; the difference in total energy equals the potential energy into the static field. The distance between the turning points is about 5×10^3 a.u., which rationalizes the splitting of 5.8 meV in our field of 220 V cm^{-1} .

In conclusion, we report on momentum distributions of electrons in HCP ionization studies starting from high-lying Rydberg states with an energy just below the saddle point energy. At low kick strength, ionization involves a core scattering process. At high kick strengths, the experiment and classical calculations reveal that ionization is determined by the first intense HCP excitation. The asymptotic properties of the electron are affected in a postionization process by the negative tail that follows the

positive HCP. For most experiments, the influence of the tail can be neglected. HCP excitation is still well suited for manipulating and controlling bound Rydberg electrons, with classical round-trip times that are shorter than the duration of the tail. We show that the tail is dominating when it can interact with ionized, escaped electrons.

We thank C. Nicole, F. Roşca-Prună, M. Yemtsova, and S. Zamith for help at different stages of the experiment. We thank E. Springate, S. Asseev, and A. Buyserd for the femtosecond laser. We acknowledge EU-Network COCOMO, HPRNT-CT-1999-00129. The work described in this paper is part of the research program of the FOM and was made possible by the financial support from NWO. F. Robicheaux was supported by the National Science Foundation.

-
- [1] B. B. Hu, J. T. Darrow, X.-C. Zhang, D. H. Auston, and P. R. Smith, *Appl. Phys. Lett.* **56**, 886 (1990); B. B. Hu, X.-C. Zhang, and D. H. Auston, *Phys. Rev. Lett.* **67**, 2709 (1991); D. You, R. R. Jones, P. H. Bucksbaum, and D. R. Dykaar, *Opt. Lett.* **18**, 290 (1993).
 - [2] R. R. Jones, D. You, and P. H. Bucksbaum, *Phys. Rev. Lett.* **70**, 1236 (1993).
 - [3] C. O. Reinhold, M. Welles, H. Shao, and J. Burgdörfer, *J. Phys. B* **26**, L659 (1993).
 - [4] A. Bugacov, B. Piraux, M. Pont, and R. Shakeshaft, *Phys. Rev. A* **51**, 1490 (1995).
 - [5] F. Robicheaux, *Phys. Rev. A* **56**, R3358 (1997).
 - [6] I. Bersons and A. Kulsh, *Phys. Rev. A* **59**, 1399 (1999); I. Bersons and A. Kulsh, *Phys. Rev. A* **60**, 3144 (1999).
 - [7] N. E. Tielking, T. J. Benschky, and R. R. Jones, *Phys. Rev. A* **51**, 3370 (1995).
 - [8] C. Wesdorp, F. Robicheaux, and L. D. Noordam, *Phys. Rev. Lett.* **87**, 083001 (2001).
 - [9] A. T. J. Eppink and D. H. Parker, *Rev. Sci. Instrum.* **68**, 3477 (1997).
 - [10] A. Kohlhaase and S. Kita, *Rev. Sci. Instrum.* **57**, 2925 (1986).
 - [11] C. Bordas, *Phys. Rev. A* **58**, 400 (1998).
 - [12] C. Nicole, I. Sluimer, F. Roşca-Prună, M. Warntjes, M. Vrakking, C. Bordas, F. Texier, and F. Robicheaux, *Phys. Rev. Lett.* **85**, 4024 (2000); C. Nicole, H. L. Offerhaus, M. J. J. Vrakking, F. Lepine, and C. Bordas, *Phys. Rev. Lett.* **88**, 133001 (2002).
 - [13] H. L. Offerhaus, C. Nicole, F. Lépine, C. Bordas, F. Roşca-Prună, and M. J. J. Vrakking, *Rev. Sci. Instrum.* **72**, 3245 (2001).
 - [14] A. Wetzels, A. Gürtler, F. Robicheaux, C. Dinu, H. G. Müller, M. J. J. Vrakking, and W. J. van der Zande (to be published).
 - [15] R. B. Vrijen, G. M. Lankhuijzen, and L. D. Noordam, *Phys. Rev. Lett.* **79**, 617 (1997).